

Ligand-based photooxidations of dithiomaltolato complexes of Ru(II) and Zn(II): photolytic CH activation and evidence of singlet oxygen generation and quenching†‡

Cite this: *Dalton Trans.*, 2014, **43**, 11548

Britain Bruner,^a Malin Backlund Walker,^b Mukunda M. Ghimire,^c Dong Zhang,^d Matthias Selke,^d Kevin K. Klausmeyer,^a Mohammad A. Omary^c and Patrick J. Farmer^{*a,b}

The complex $[\text{Ru}(\text{bpy})_2(\text{ttma})]^+$ (bpy = 2,2'-bipyridine; ttma = 3-hydroxy-2-methyl-thiopyran-4-thionate, **1**, has previously been shown to undergo an unusual C–H activation of the dithiomaltolato ligand upon outer-sphere oxidation. The reaction generated alcohol and aldehyde products **2** and **3** from C–H oxidation of the pendant methyl group. In this report, we demonstrate that the same products are formed upon photolysis of **1** in presence of mild oxidants such as methyl viologen, $[\text{Ru}(\text{NH}_3)_6]^{3+}$ and $[\text{Co}(\text{NH}_3)_5\text{Cl}]^{2+}$, which do not oxidize **1** in the dark. This reactivity is engendered only upon excitation into an absorption band attributed to the ttma ligand. Analogous experiments with the homoleptic $\text{Zn}(\text{ttma})_2$, **4**, also result in reduction of electron acceptors upon excitation of the ttma absorption band. Complexes **1** and **4** exhibit short-lived visible fluorescence and long-lived near-infrared phosphorescence bands. Singlet oxygen is both generated and quenched during aerobic excitation of **1** or **4**, but is not involved in the C–H activation process.

Received 1st April 2014,
Accepted 23rd May 2014

DOI: 10.1039/c4dt00961d

www.rsc.org/dalton

Introduction

Much effort has gone into the development of new photochemical dyes which induce electron transfer reactions upon exposure to light, for use in dye sensitized solar cell (DSSC) and other photochemical applications.¹ Most commonly used are luminescent compounds based on the well-known families of $\text{Ru}(\text{diimine})_x$ and porphyrin-based species, which form long-lived triplet states (³ES) that undergo facile electron-transfer reactions.² In particular, the $[\text{Ru}(\text{diimine})_2\text{L}]^{2+}$ family of complexes have been extensively studied due to photochemical

redox reactivity involving electron transfer reactions from long-lived luminescent states.^{3–8}

Anthocyanin, a red dye found in many berries, was shown to have an unusually good efficiency as a DSSC dye when chelated to the surface of titania.⁹ Chemically similar hydroxypyronone chelates such as maltol have been studied for use as diagnostic tools,¹⁰ anticancer drugs,^{11,12} and metal transport.^{13–15} Thiomaltol,¹⁶ in which the pyronal ketone is replaced with a thione, has been used for similar applications.^{17,18} A ring substituted derivative, 3-hydroxy-2-methyl-4H-thiopyran-4-thione, dithiomaltol or Httma, was first reported by Brayton, and displayed unusual aromaticity characterized by a downfield shift in the vinylic proton peaks in the ¹H NMR.¹⁹

Recently we reported that the bis-bipyridyl Ru complex of dithiomaltol, $[\text{Ru}(\text{bpy})_2(\text{ttma})][\text{PF}_6]$ or **1**, undergoes C–H activation at a pendant alkyl position upon electrochemical or bulk oxidation, yielding $[\text{Ru}(\text{bpy})_2(\text{ttma-alcohol})]^+$ **2** and $[\text{Ru}(\text{bpy})_2(\text{ttma-aldehyde})]^+$ **3** as products, Scheme 1.²⁰ In this report we examine the photo-initiation of similar oxidative reactivity for compound **1** and the homoleptic $\text{Zn}(\text{ttma})_2$ complex, **4**, using flash quench methodology,²¹ employing electron acceptors 4,4'-dimethyl-1,1'-trimethylene-2,2'-dipyridinium (DTDP²⁺), 1,1'-dimethyl-4,4'-bipyridinium (MV²⁺), $\text{Co}(\text{NH}_3)_5\text{Cl}^{2+}$, $\text{Ru}(\text{NH}_3)_6^{3+}$, and 2,3-dichloro-5,6-dicyano-1,4-benzoquinone (DDQ), Scheme 2.

^aDepartment of Chemistry and Biochemistry, Baylor University, Waco, Texas 76798, USA. E-mail: Patrick_Farmer@baylor.edu

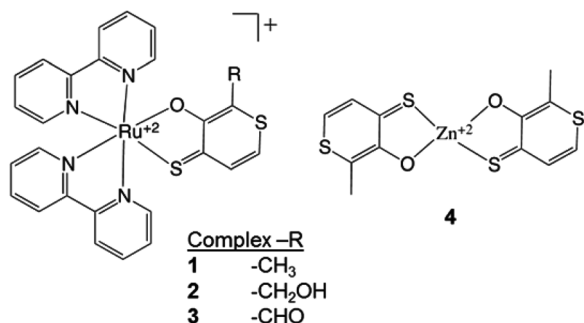
^bDepartment of Chemistry, University of California, Irvine, Irvine, CA 92697, USA

^cDepartment of Chemistry, University of North Texas, Denton, Texas 76203, USA

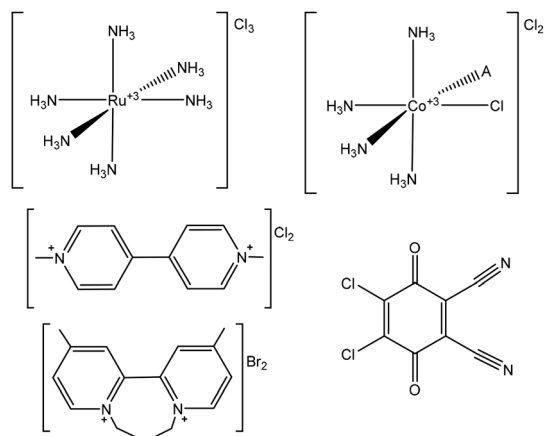
^dDepartment of Chemistry and Biochemistry, California State University, Los Angeles, Los Angeles, CA 90032, USA

†This paper is dedicated to the memory of Prof. Oussama El-Bjeirami, who contributed to this work.

‡Electronic supplementary information (ESI) available: Including crystallographic data for Httma, ¹H NMR comparison of compounds **1**, **3** and **4**, MS analysis of photolysis products, and steady state quenching and singlet oxygen quenching experiments. CCDC 1000544. For ESI and crystallographic data in CIF or other electronic format see DOI: 10.1039/c4dt00961d



Scheme 1 Complexes investigated in this work.



Scheme 2 Oxidative quenchers used.

Results and discussion

Synthesis and characterization of Httma and Zn(ttma)₂, 4

Coordination complexes of Httma with metal ions are typically synthesized by deprotonation at room temperature or heating at high temperature in polar protic solvents.^{14,15} Both methods were used in synthesizing previously reported compounds [Ru(bpy)₂(ttma)]PF₆, **1**,²² and Zn(ttma)₂, **4**.²³ X-ray diffractometry was used to determine the structure of Httma, shown in Fig. 1, and of **4** in Fig. 2. Details of the crystal parameters, data collection, and refinement are summarized in Table 1. The structures of **1** and **3** were previously reported;²⁰ bond length data are compared in the ESI.†

Ligand constraint in compound **4** distorts metal-centered geometry with O(1)–Zn(1)–S(3) angle at 123.38(6)° and

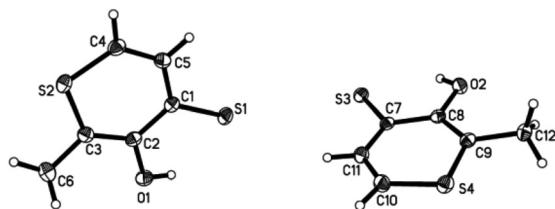


Fig. 1 Crystal structure of Httma, two molecules are within the unit cell.

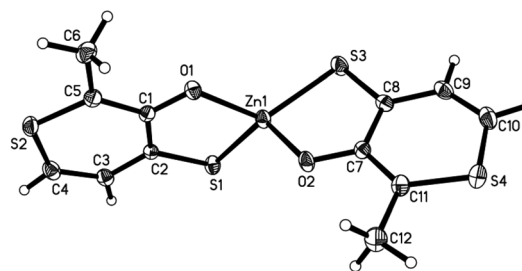
Fig. 2 Crystal structure of Zn(ttma)₂, **4**.

Table 1 Crystallographic data

	Httma	4
Empirical formula	C ₆ H ₆ OS ₂	C ₁₃ H ₁₁ C ₁₃ O ₂ S ₄ Zn
Formula mass	158.23	499.18
<i>a</i> (Å)	5.3629(4)	7.5568(9)
<i>b</i> (Å)	8.6723(7)	25.901(4)
<i>c</i> (Å)	13.5524(11)	7.6967(10)
α (°)	90.00	73.404(3)
β (°)	114.730(4)	79.141(3)
γ (°)	90.00	75.735(3)
<i>V</i> (Å ³)	1368.3(3)	921.33(16)
<i>Z</i>	8	2
Crystal system	Monoclinic	Triclinic
Space group	<i>P</i> 2(1)/ <i>c</i>	<i>P</i> 1̄
<i>T</i> (K)	110(2)	110(2)
<i>D</i> _{calcd} (g cm ⁻³)	1.536	1.536
μ (mm ⁻¹)	0.684	2.224
$2\theta_{\max}$ (°)	28.3	28.32
Reflections measured	3347	4491
Reflections used	2983	3850
Data/restraints/parameters	2983/0/173	2850/0/210
<i>R</i> ₁ [<i>I</i> > 2 σ (<i>I</i>)]	0.0317	0.0383
<i>wR</i> ₂ [<i>I</i> > 2 σ (<i>I</i>)]	0.0757	0.0993
<i>R</i> (<i>F</i> ² _o) (all data)	0.0366	0.0486
<i>R</i> _w (<i>F</i> ² _o) (all data)	0.0799	0.1199
GOF on <i>F</i> ²	1.046	1.091

Table 2 Structural data of complex **4**

Bond (Å)	Angle (°)		
Zn(1)–O(1)	1.957(2)	O(1)–Zn(1)–O(2)	106.80(9)
Zn(1)–O(2)	1.979(2)	O(1)–Zn(1)–S(3)	123.38(6)
Zn(1)–S(3)	2.2871(8)	O(2)–Zn(1)–S(3)	88.79(6)
Zn(1)–S(1)	2.2968(8)	O(1)–Zn(1)–S(1)	89.48(6)
		O(2)–Zn(1)–S(1)	119.95(7)
		S(3)–Zn(1)–S(1)	129.30(3)

O(2)–Zn(1)–S(3) at 88.79(6)°. The dihedral angle between the two ligands is 93° while the bite angles of the ligands are <90°. Summary of selected bond lengths, angles, and interatomic distances for compound **4** are given in Table 2.

Electrochemical measurements

The ground state redox properties of Httma, **1** and **4** were assessed using cyclic voltammetry, shown in Fig. 3 and Table 3. The Httma undergoes a characteristic irreversible reduction at –0.98 V NHE, with similar reductions seen at

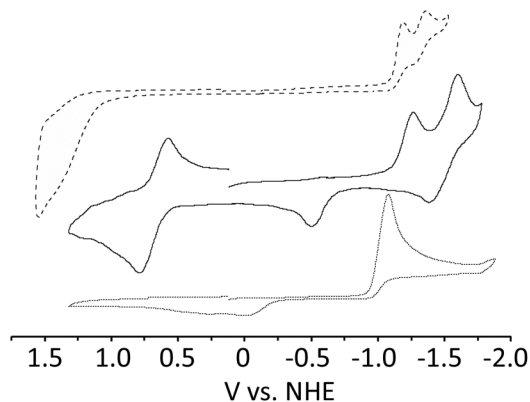


Fig. 3 Cyclic voltammograms of **1** (solid), **4** (dashed), and Httma (dotted) in anhydrous CH_3CN with 0.1 M TBAPF_6 as the supporting electrolyte on glassy carbon disc electrode, scan rate 100 mV s^{-1} .

Table 3 Electrochemical data^a

	E'_{Ox}	E'_{Red}
Httma	-0.156(ir)	-0.969(ir)
1	+0.693	-1.117(ir)
		-1.488
4	+1.200(ir)	-1.119(ir)
		-1.359

^a All potentials adjusted vs. NHE in CH_3CN , 0.1 M TBAPF_6 .

ca. -1.12 V for the metal complexes; a related oxidation wave is seen on the return scan, at *ca.* -0.1 V for Httma, and -0.4 and -0.6 V for compounds **4** and **1**, respectively. Compound **1** also displays quasi-reversible oxidation at 0.7 V, assigned to the $\text{Ru}^{2+/3+}$ couple, and reduction at *ca.* -1.5 V, assigned to the bipyridine moieties.

Photophysical and photochemical studies

The normalized absorption spectra of metal complexes **1**, **4** and well-known $\text{Ru}(\text{bpy})_3^{2+}$ are compared in Fig. 4. The absorp-

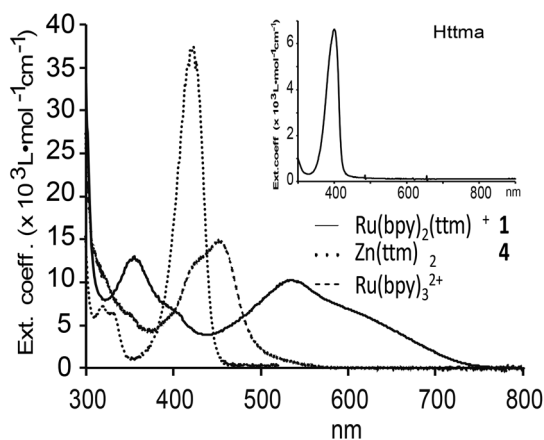


Fig. 4 Comparison of normalized absorption spectra of $[\text{Ru}(\text{bpy})_2\text{-ttma}]^+$ (—), $\text{Zn}(\text{ttma})_2$ (···) and $\text{Ru}(\text{bpy})_3^{2+}$ (---) molar extinction coefficient ($\text{L mol}^{-1} \text{cm}^{-1}$). Inset: of Httma over same range.

Table 4 Complex absorption and emission data

Complex	Absorption max (nm)	Ext. coeff. ($\text{M}^{-1} \text{cm}^{-1}$)	Emission (nm)	Lifetime (μs)
1	352	16 400	420	0.01
			1080	8.50
4	537	12 100	450	0.005
	422	37 100	1275	75.0

tion of metal-coordinated ttma is demonstrated by the band at 420 nm in the spectrum of $\text{Zn}(\text{ttma})_2$, **4**. Several other ttma complexes show similar ligand-based absorption bands with extinction coefficients on the order of 10 to $20 \times 10^3 \text{ L mol}^{-1} \text{cm}^{-1}$ per ttma ligand.²³ The spectrum of **1** shown exhibits mid-range bands from 450 to 750 nm which are significantly shifted and broadened in comparison to the analogous bands of $[\text{Ru}(\text{bpy})_3]^{2+}$. These and other determined photochemical properties of complexes **1** and **4** are given in Table 4.

Excitation of **1** in CH_3CN solution at wavelengths $>400 \text{ nm}$ generates no observable emissions, but excitation into the 355 nm band obtains a short-lived fluorescence ($\lambda_{\text{em}} = 420 \text{ nm}$, $\tau_{\text{em}} = 10 \text{ ns}$) which increases in intensity *ca.* 100 fold at 77 K. Measurements in the near IR identified a phosphorescent emission from this excitation, with maximum at $\lambda_{\text{em}} = 1080 \text{ nm}$ and $\tau_{\text{em}} = 8.5 \mu\text{s}$, Fig. 5.

Addition of MV^{2+} to anaerobic solutions of **1** significantly decreases the intensity of the 1080 nm emission (SM) but does not shorten its lifetime. Excitation of **4** into the 422 nm band

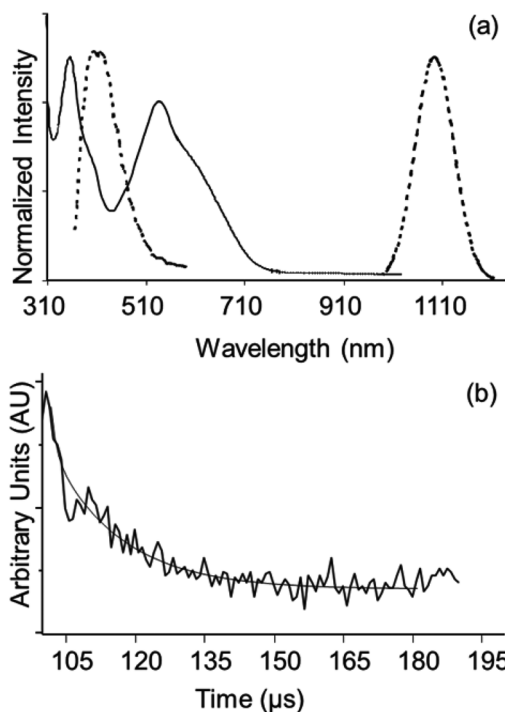


Fig. 5 (a) Normalized absorption (solid line) and emission (dotted) spectra for compound **1** in CH_3CN . (b) Emission transient trace from excitation at 352 nm, at 1080 nm ($\tau_{\text{em}} = 8.5 \mu\text{s}$).

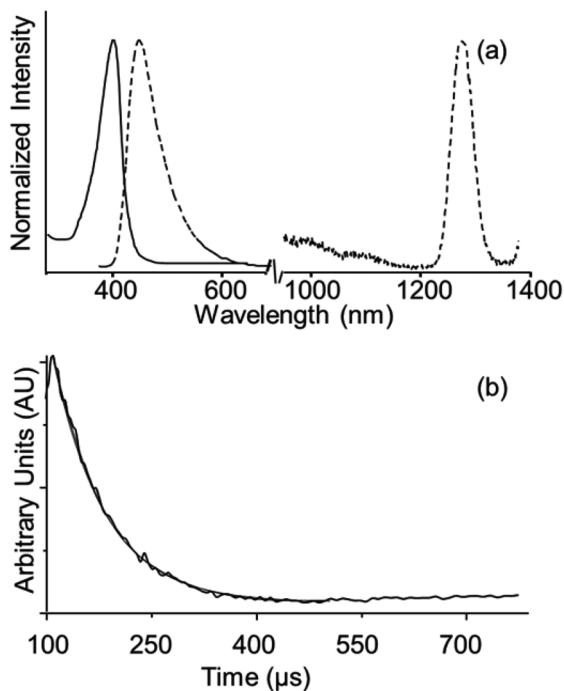


Fig. 6 (a) Normalized absorption (solid line) and emission (dotted) spectra for **4** in CH_3CN . (b) Emission transient trace at 1275 nm and data fit (dotted line, $\tau_{\text{em}} = 75 \mu\text{s}$), from excitation at 400 nm.

($\epsilon = 37\,100 \text{ M}^{-1} \text{ cm}^{-1}$) obtains a short lived ($\tau \sim 5 \text{ ns}$) emission with maximum at 450 nm, which is quenched in the presence of excess MV^{2+} . Complex **4** has a phosphorescent emission at 1275 nm, $\tau_{\text{em}} = 75 \mu\text{s}$, Fig. 6.

Bulk oxidations by flash quench photolysis

Initial flash quench experiments at room temperature showed that irradiation of **1** in $\text{CH}_3\text{CN}-\text{CH}_3\text{OH}$ mixtures with a large 200-fold excess of the electron-acceptor methyl viologen, MV^{2+} , using a Hg lamp and a 400 nm low-pass filter generates a blue product solution characteristic of reduced MV^+ in *ca.* 15 min; addition of basic water to the product solution gives $[\text{Ru}(\text{bpy})_2(\text{ttma-alcohol})]^+$ **2** in *ca.* 10% yield by ESI-MS analysis, Fig. 7.

Analogous irradiation experiments using a 400 nm high-pass filter showed no observable changes. Photolysis of $[\text{Ru}(\text{bpy})_2(\text{ttma})]^+$ at room temperature in H_2O but in the absence of an electron transfer agent at room temperature leads to displacement of the ttma ligand to form the $[\text{Ru}(\text{bpy})_2(\text{H}_2\text{O})(\text{OH})]^+$ complex, as previously reported for analogous complexes (ESI SM3[†]).^{24,25} Subsequently, all photolysis experiments using complex **1** were conducted at 5 °C in the absence of water, with addition of basic water afterwards.

Bulk photolysis of CH_3CN solutions of **1** in the presence of varied potential electron acceptors $\text{Co}(\text{NH}_3)_5\text{Cl}_3$ and $\text{Ru}(\text{NH}_3)_6\text{Cl}_3$ generated color changes indicative of reduction of the oxidants; the reactions were quenched with the addition of basic water after photolysis. LCMS of the product solutions from these reactions after 20 minutes showed distinct reten-

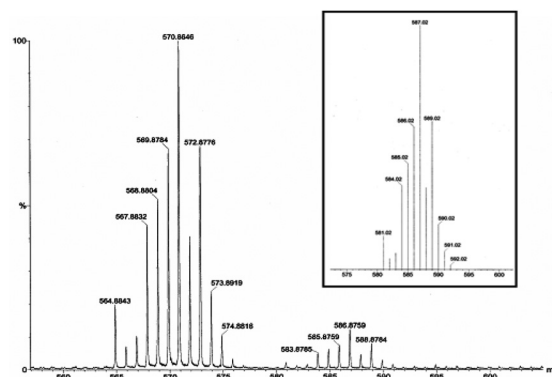


Fig. 7 ESI-MS spectrum of a sample generated by photoexcitation of an anaerobic solution of $[\text{Ru}(\text{bpy})_2(\text{ttma})]^+$ and MV^{2+} in $\text{CH}_3\text{CN}-\text{CH}_3\text{OH}$ following the addition of 0.1 M NaOH. The species formed is $[\text{Ru}(\text{bpy})_2(\text{ttma-alcohol})]^+$ ($m/z = 587$). Inserted in the box is the predicted isotopic envelope for $[\text{Ru}(\text{bpy})_2(\text{ttma-alcohol})]^+$.

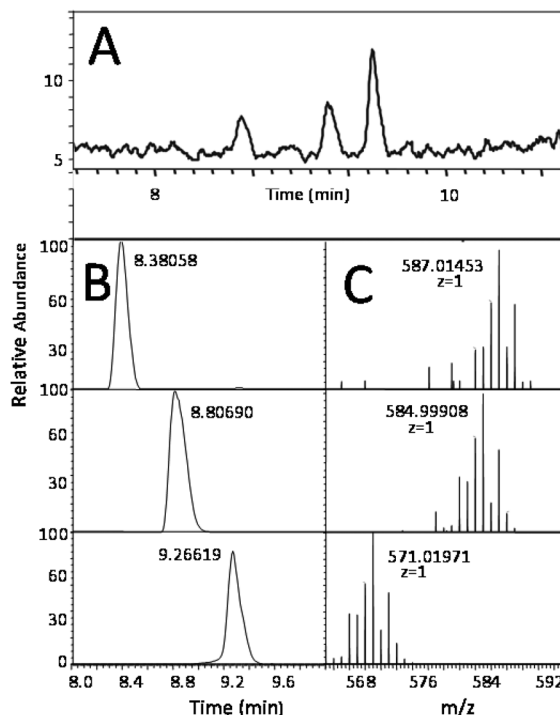


Fig. 8 LCMS analysis of product solution after photolysis of **1** for in presence of $\text{Ru}(\text{NH}_3)_6\text{Cl}_3$ at 1:1.1 stoichiometry in CH_3CN . (A) Region of the total ion current chromatogram showing product peaks; selective ion mass chromatogram peaks (B) and corresponding ion mass spectra ($m/z = 1$) (C) of $[\text{Ru}(\text{bpy})_2(\text{ttma-OH})]^+$, $[\text{Ru}(\text{bpy})_2(\text{ttma=O})]^+$, and $[\text{Ru}(\text{bpy})_2(\text{ttma})]^+$.

tion times approximately 30 s apart for the complexes **1-3**, Fig. 8. Selected ion monitoring (SIM) was used to assign total ion current (TIC) peaks to the products separated.

Definitive characterization of the C-H oxidation products was obtained by chromatographic separations following analogous larger scale reactions over 3 h, Table 5. ^1H NMR characterization of the isolated **3** was used to confirm the structural

Table 5 Photolysis yields

Oxidant	% Yield ^a (isolated ^b)		
	1	2	3
MV ²⁺	73 (61.4)	15	12 (7.15)
Ru(NH ₃) ₆ ³⁺	45 (77.7)	9	34 (19.3)
Co(NH ₃) ₅ ³⁺	45 (45.7)	16	39 (50.4)

^a LCMS yields using *ca.* 1.1 fold excess of oxidant, after 20 min.

^b Isolated yields using *ca.* 1.4 fold excess oxidant, 200 fold for MV²⁺, after 3 h.

Table 6 Reduction potential vs. photolysis yields

Oxidant	<i>E</i> ^{0'} (V NHE)	Yield (%)	Zn ^a (+/–)
DTDP ²⁺	–0.691 (ref. 26a)	—	–
MV ²⁺	–0.440 (ref. 26b)	27	–
Ru(NH ₃) ₆ ³⁺	–0.159 (ref. 26c)	43	+
Co(NH ₃) ₅ Cl ²⁺	0.341 (ref. 26c)	55	+
DDQ	0.754 (ref. 26d)	—	+

^a Photoreduction by **4** indicated by +/–.

assignment (ESI SM4†) by comparison to the original reported spectra as well as to that of new samples of **3** generated by dark oxidation of **1** using the organic oxidant DDQ. Yields of the alcohol **2** were not obtained due to its decomposition during aerobic purification and manipulations.

Bulk photochemical oxidation of the homoleptic Zn complex **4** was assayed in a similar manner. Photolysis of **4** in the presence of DTDP²⁺ or MV²⁺ did not produce noticeable color changes indicative of irreversible reduction. Photolysis in the presence of Co(NH₃)₅Cl, Ru(NH₃)₆Cl₃ and DDQ initiated a change in color of the reaction mixtures indicating reduction of the oxidants. Analysis of the photolyzed solutions by MS showed a mixture of oligomeric C_xH_yO_z⁺ species as the main components (ESI SM5†); the structures of these species have not been determined. The potential dependence of the oxidative flash quench yields are shown in Table 6. The trend in increasing *E*^{0'} and yield across the photo-oxidants follows as Co(III) > Ru(III) > MV²⁺ > DTDP²⁺.

Singlet O₂ sensitization/desensitization

The near IR emissions of both **1** and **4** are quenched in the presence of ³O₂, generating ¹O₂. Fig. 9 shows the near IR emission signals of **1** and **4** as well as a longer lived emission due to the ¹O₂ generated. Extrapolating the time-resolved singlet oxygen emission signal to *t* = 0 yields a value of $\Phi^{\Delta} = 0.14 \pm 0.02$ for **1** and 0.64 ± 0.06 for **4** in CD₃OD, with C₆₀ and Rose Bengal used as references. The ground state of complex **1** also functions as an efficient quencher of singlet oxygen; in Fig. 9, the lifetime of the singlet oxygen signal in MeOD is shortened from 170 μ s to 67 μ s due to quenching by ground-state [Ru(bpy)₂(ttma)]⁺; the lifetime of singlet oxygen is unaffected by compound **4**. Additional data is given in ESI (SM7 and SM8†). The total rate constant for removal of ¹O₂ by ground state

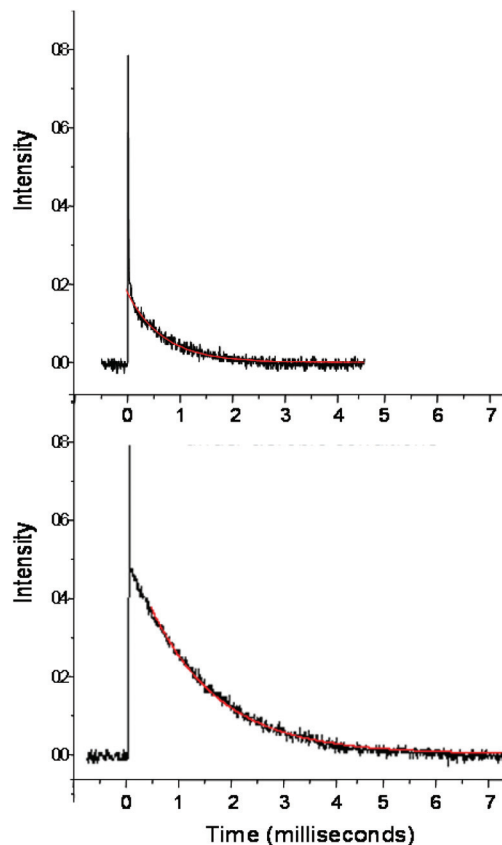


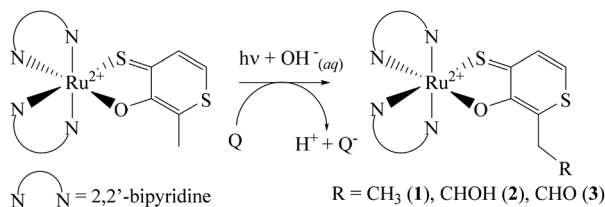
Fig. 9 Singlet oxygen emission transient trace in the near IR obtained upon excitation of **1** (top) and **4** (bottom) at 355 nm under aerobic conditions. The inset lines represent the best exponential fits for the long-lived emission due to singlet oxygen. The sharp emission peaks are due to the inherent emissions of the complexes.

complex **1** in CD₃OD was determined by time-resolved singlet oxygen luminescence quenching experiments to be $5.0 \pm 0.2 \times 10^8 \text{ M}^{-1} \text{ s}^{-1}$.

Discussion

Previous work demonstrated that bulk or electrochemical oxidation of **1** generated a darkly colored species, which reacted with water or other nucleophiles to give products oxidized at the pendant methyl. We noted that the ring proton resonances in ¹H NMR spectra of the Ru-bound ttma suggest it to possess aromaticity. We rationalized the C–H oxidation as a result of thiopyrillium character in the oxidized ttma ligand.^{28–30}

In this work we investigated the initiation of this oxidative chemistry by photo-excitation, analogous to the well-known flash-quench reactivity of Ru(bpy)₃²⁺.^{5,21} Our goal was to initiate the oxidation of **1** by flash quench methods, *i.e.* to excite the complex in the presence of an electron acceptor and look for the C–H oxidation products. No reactivity was seen upon excitation into the broad visible absorption of **1**, but excitation with wavelengths below 400 nm did induce electron transfer reactivity, Scheme 3. Good yields of the same products



Scheme 3 Oxidative quenching reaction.

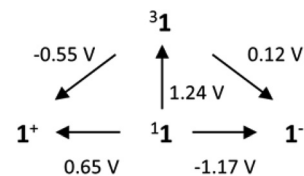
formed by ground state oxidation were obtained using high potential electron acceptors during flash-quench reactions.

The MLCT-like absorptions of **1** are significantly broader than that of $[\text{Ru}(\text{bpy})_3]^{2+}$, suggesting strong electronic coupling between the Ru(II) and ttma ligand, but no analogous luminescence is obtained. We found excitation into a band tentatively assigned to the ttma ligand generates a short-lived singlet emission and a long-lived emission in the near IR, more characteristic of organic triplet phosphorescence. The homoleptic Zn complex **4** was used as a simple test of these assignments; and excitation of **4** into the analogous ttma band at 422 nm did indeed generate similar fluorescent and phosphorescent emissions. Photo-excitation of Httma alone yields no products, thus coordination to a metal center is essential for the observed electron transfer chemistry to take place.

The possible involvement of trace oxygen contamination was also investigated. Both compounds **1** and **4** are efficient sensitizers of singlet oxygen; compound **1** also functions as an efficient singlet oxygen desensitizer. These may be examples of singlet oxygen sensitization by a simple Forster mechanism, *i.e.* by an emission/absorption overlap. Excitation of **1** under air generates no observable yields of the C–H activation products **2** or **3**, indicating that singlet oxygen itself is not involved in the C–H activation process, consistent with the known reactivity of $^1\text{O}_2$.³⁰

Thus excitation of **1** produces a photostate which is capable of irreversibly reducing MV^{2+} ($E^{0'}$ = –440 mV NHE) but not DTDP^{2+} ($E^{0'}$ = –691 mV). This highly reducing photostate must be relatively short-lived, as any species capable of reducing MV^{2+} should quantitatively reduce both $\text{Ru}(\text{NH}_3)_6^{3+}$ and $\text{Co}(\text{NH}_3)_5\text{Cl}^{2+}$. Also notable is that an excess of MV^{2+} effectively quenches the emissions of the homoleptic Zn adduct **4** but does not irreversibly oxidize it, as occurs in analogous photolysis experiments with $\text{Ru}(\text{NH}_3)_6^{3+}$ and $\text{Co}(\text{NH}_3)_5\text{Cl}^{2+}$ quenchers. Thus complex **1** is a more powerful photo-reductant than **4**, roughly following the observed ground state reduction potentials which are assigned to the ttma moiety in these species.

A simple thermodynamic cycle denoting possible electron transfer reactions of the phosphorescent state of **1** is shown in Scheme 4, and comparable data for **4** is given in Table 7. The short-wavelength edges of the emissions were used to estimate the energy between the lowest triplet state and ground state.³¹ From these values, the excited state of **1** is predicted to be competent to reduce MV^{2+} while that of **4** is not, as is observed. But similarly, the triplet excited state of **4** should not reduce $\text{Ru}(\text{NH}_3)_6^{3+}$, counter to experiment. As previously noted, the



Scheme 4 Photochemical cycles based on triplet reactivity.

Table 7 Thermodynamic estimates for triplet energies

Complex	E^{00} (nm)	E^{00} (eV)	E^*_{Ox} (V NHE)	E^*_{Red} (V NHE)
1	1000	1.24	–0.55	0.12
4	1220	1.02	0.18	–0.17

^a Estimated from edge of emission band.

addition of MV^{2+} to anaerobic solutions of **1** prior to photo-excitation significantly decreases the intensity of the near IR emission without shortening its lifetime. This implies that once formed, the emissive state is not involved in the electron transfer, *i.e.*, the photo-state which reduces MV^{2+} must precede the phosphorescent state.

Thus, the nature of the reductive excited states of compounds **1** and **4** remain obscure. Certain aromatic thiones demonstrate unusual phosphorescence,^{32–34} for example T_2 emissions have been described for uncomplexed aromatic thiones, as well as T_1 – T_2 energy inversion caused by interactions of the excited state with solvent.^{35–37} A thione similar to Httma, 3-hydroxyflavothione demonstrates a long-lived emission when coordinated to transition metals with paired electrons,^{35,36} very similar to the behavior described here.

Experimental

Materials

The dithiomaltol ligand, $[\text{Ru}(\text{bpy})_2(\text{ttma})]\text{PF}_6$, $\text{Zn}(\text{ttma})_2$ and 4,4'-dimethyl-1,1'-trimethylene-2,2'-dipyridinium dibromide, $(\text{DTDP})\text{Br}_2$, were prepared according to published procedures.^{22,23} Electron acceptors 1,1'-dimethyl-4,4'-bipyridinium dichloride (MV^{2+}) Cl_2 , $\text{Co}(\text{NH}_3)_5\text{Cl}_3$, $\text{Ru}(\text{NH}_3)_6\text{Cl}_3$, and 2,3-dichloro-5,6-dicyano-1,4-benzoquinone (DDQ) and all other chemicals used were purchased from Sigma-Aldrich. Air-sensitive manipulations were carried out using Schlenk techniques or in an anaerobic dry glovebox.

Physical measurements

Electronic adsorption spectra were recorded by Perkin Elmer Lambda 900 or a Hewlett Packard 8453 Diode Array spectrophotometers. Emission and excitation spectra were recorded on a Hitachi F-4500 fluorescence spectrometer. All photochemical reactions were performed anaerobically in quartz fluorescence cells or sealed jacketed beakers.

Crystallographic data was collected on crystals with dimensions $0.31 \times 0.18 \times 0.08$ mm for **1**, $0.28 \times 0.17 \times 0.14$ mm for **2**, $0.28 \times 0.17 \times 0.14$ mm for **4**, and $0.31 \times 0.18 \times 0.08$ mm for Httma. Data was collected at 110 K on a Bruker X8 Apex using Mo-K radiation ($\lambda = 0.71073$ Å). All structures were solved by direct methods after correction of the data using SADABS.^{37–39} All the data were processed using the Bruker AXS SHELXTL software, version 6.10.⁴⁰

Redox potentials were measured by cyclic voltammetry under anaerobic conditions using a CHI-760B potentiostat in dry-degassed CH_3CN with 0.1 M tetrabutylammonium hexafluorophosphate (TBAPF_6) as the supporting electrolyte. The cells consisted of a glassy-carbon working electrode (3.0 mm dia.), a AgCl coated Ag reference wire, and a coiled Pt wire auxiliary electrode. Measured potentials were corrected using a ferrocene standard, with the Fc/Fc^+ couple set to 642 mV NHE.

Large-scale photolysis experiments were carried out using an Oriol Apex Quartz Tungsten Halogen Source with a 150 W Xe Arc Lamp and filter accessories. Samples were stirred under N_2 at 5 °C for 3 h. Smaller scale photolysis were performed anaerobically under N_2 at 5 °C in a 3 mL anaerobic quartz fluorescence cells for 45 min and worked up on bench top.

Mass spectra were collected from an Accela Bundle Liquid Chromatograph (LC) coupled to a Thermo Electron Linear Trap Quadrupole Orbitrap Discovery mass spectrometer (Orbitrap) using positive electrospray ionization (+ESI) or by Direct Infusion (DI) with +ESI. Data were collected and processed using Xcalibur v.2.0.7 software. Standards for LC separation were used to calibrate reaction yields for compounds **1** and **3**. Isolated yields were carried out by column-chromatography inside a glove box. Samples were collected and stored under inert atmosphere, removed from the glovebox, dried under vacuum, and returned to the glovebox to record mass and prepare samples for ^1H NMR.

Near IR emissions were measured in acetonitrile (CH_3CN) with a Photon Technology International (PTI) QuantaMaster Model QM-4 scanning spectrofluorometer equipped with a 75-watt xenon lamp, emission and excitation monochromators, excitation correction unit, and a near-infrared (NIR) photomultiplier tube (PMT) from Hamamatsu. Lifetimes were collected using a pulsed Xenon source with a pulse repetition rate of 300 pulse s^{-1} and a PTI-supplied Gated Voltage-Controlled Integrator to interface to the NIR PMT.

Synthesis of dithiomaltol, Httma

Dithiomaltol was synthesized using a modification of previously reported methods.⁹ A sample of 3-hydroxy-2-methyl-4-pyrone (maltol, 1.0 g, 7.93 mmol) was combined with 1.1 eq. of hexamethyldisiloxane (HMDO, 1.85 mL, 87.2 mmol) in 60 mL of anhydrous toluene and gently heated for 30 min. A sample of Lawesson's Reagent (3.53 g, 87.3 mmol) was then added before fitting the reaction flask with a condenser, and heated to reflux under nitrogen for 1.5 h. A black precipitate was removed by vacuum filtration, and the filtrate was concentrated to give a dark brown solid. The product was purified by silica flash column chromatography eluting with 4% CH_3OH

in CH_2Cl_2 , as a bright orange band. After removal of solvent by reduced atmosphere, an orange solid was isolated, which gave dithiomaltol as orange iridescent flakes. Yield: 70%. Slow evaporation of the solid in hexanes gave orange needles suitable for X-ray diffraction studies. ^1H NMR (500 MHz, CDCl_3): δ 9.34 (s, 1H), 8.17 (d, 1H), 7.51 (d, 1H), 2.49 (s, 3H); ESI MS: m/z , 159 ($[\text{M} + \text{H}]^+$); UV-vis: CH_3CN , λ_{max} (ϵ in $\text{L mol}^{-1} \text{cm}^{-1}$) 221 ($\epsilon = 4300$), 285 ($\epsilon = 1700$), 397 ($\epsilon = 6600$).

Synthesis of $\text{Zn}(\text{ttma})_2$, **4**

Httma (0.097 g, 0.613 mmol) was added to 19 mL of a stirred 0.029 M NaOH in a CH_3OH solution turning it a red color. Five minutes later ZnCl_2 (0.040 g, 0.291 mmol) and 20 mL of DI H_2O was added to the stirred solution, a light yellow precipitates formed immediately, and the reaction was left to stir overnight. Filtering the reaction solution yielded 0.092 g (83%) of a yellow solid. The compound was crystallized in CH_2Cl_2 by slow evaporation to produce samples suitable for X-ray diffraction. ^1H NMR (500 MHz, CDCl_3): δ 2.64 (s, 6 H, $-\text{CH}_3$), 7.58 (d, 2 H, $J = 9.1$ Hz), 8.43 (d, 2 H, $J = 9.1$ Hz). Electrospray MS: 401 ($[\text{M} + \text{Na}]^+$). Anal. Calcd for $\text{H}_{10}\text{C}_{12}\text{S}_4\text{O}_2\text{Zn}$: C, 37.90; S, 33.76; H, 2.65. Found: C, 37.70; S, 33.66; H, 2.63.

Chemical oxidation of $[\text{Ru}(\text{bpy})_2\text{ttma}][\text{PF}_6]$ with DDQ

The complex $[\text{Ru}(\text{bpy})_2(\text{ttma})][\text{PF}_6]$ (4.21 mg, 5.87 μmol) and DDQ (1.33 mg, 5.86 μmol) were placed in a 50 mL flask with 10.0 mL anhydrous CH_3CN . The flask was sealed, degassed with N_2 . The reaction was stirred for 45 min before the addition of NaOH_{aq} (1 mol eq.) after which the solvent was removed under N_2 purge and separated by column chromatography inside a glove box using alumina as the separation media and anhydrous acetonitrile as the eluent. The isolated yield of aldehyde **3** was 3.94 mg (91.9%). ESI MS: m/z 584.99. ^1H NMR (500 MHz, CD_3CN): δ 9.96 (d, $J = 1.5$, Hz, 1H), 9.18 (d, $J = 5$, Hz, 1H), 8.56 (d, $J = 5$, Hz, 1H), 8.46 (d, $J = 7.21$, Hz, 1H), 8.44 (d, $J = 8.29$, Hz, 1H), 8.43 (d, $J = 9.21$, Hz, 1H), 8.32 (d, $J = 8.3$, Hz, 1H), 8.08 (d, $J = 8.02$, 1.3, Hz, 2H), 8.05 (d, $J = 9.3$, Hz, 1H), 7.96 (d, $J = 8.03$, 1.49, Hz, 1H), 7.88 (d, $J = 5.7$, Hz, 1H), 7.79 (d, $J = 7.99$, 1.4, Hz, 1H), 7.76 (d, $J = 9.3$, 1.5, Hz, 1H), 7.62 (d, $J = 7.3$, 1.25, Hz, 1H), 7.61 (d, $J = 6.07$, Hz, 1H), 7.58 (d, $J = 7.3$, 1.3, Hz, 1H), 7.3 (d, $J = 7.31$, 1.2, Hz, 1H), 7.13 (d, $J = 7.3$, 1.3, Hz, 1H).

Large scale photochemical oxidations of $[\text{Ru}(\text{bpy})_2\text{ttma}][\text{PF}_6]$ (**1**) and of $\text{Zn}(\text{ttma})_2$ (**4**)

In a typical experiment, samples of $[\text{Ru}(\text{bpy})_2(\text{ttma})][\text{PF}_6]$ (34.9 mg, 48.8 μmol) and pentaminechlorocobalt(III) chloride, $\text{Co}(\text{NH}_3)_5\text{Cl}_3$ (13.0 mg, 51.9 μmol) were placed in a 50 mL jacketed flask with 10.0 mL anhydrous acetonitrile. The flask was sealed, degassed with N_2 , and cooled to 5 °C with a circulating cooling bath. The reaction mixture was photolyzed for 45 min with a 400 nm low-pass filter before the addition of NaOH_{aq} (1 mol eq.), after which the solvent was removed under N_2 purge and separated on an alumina column inside a glove box with anhydrous CH_3CN as eluent. The isolated yield of aldehyde **3** was 17.9 mg (50.4%). ESI MS: m/z 584.99. ^1H NMR (500 MHz, CD_3CN): δ 9.96 (d, $J = 1.5$, Hz, 1H),

9.18 (d, $J = 5$, Hz, 1H), 8.56 (d, $J = 5$, Hz, 1H), 8.46 (d, $J = 7.21$, Hz, 1H), 8.44 (d, $J = 8.29$, Hz, 1H), 8.43 (d, $J = 9.21$, Hz, 1H), 8.32 (d, $J = 8.3$, Hz, 1H), 8.08 (d, $J = 8.02$, 1.3, Hz, 2H), 8.05 (d, $J = 9.3$, Hz, 1H), 7.96 (d, $J = 8.03$, 1.49, Hz, 1H), 7.88 (d, $J = 5.7$, Hz, 1H), 7.79 (d, $J = 7.99$, 1.4, Hz, 1H), 7.76 (d, $J = 9.3$, 1.5, Hz, 1H), 7.62 (d, $J = 7.3$, 1.25, Hz, 1H), 7.61 (d, $J = 6.07$, Hz, 1H), 7.58 (d, $J = 7.3$, 1.3, Hz, 1H), 7.3 (d, $J = 7.31$, 1.2, Hz, 1H), 7.13 (d, $J = 7.3$, 1.3, Hz, 1H). Analogous experiments were carried out with MV^{2+} and $Ru(NH_3)_6Cl_3$ as described in text.

Photochemical oxidations of $Zn(ttma)_2$ follow the same procedures. As example, a mixture of **4** (12.6 mg, 33.0 μ mol) and $Co(NH_3)_5Cl_3$ (7.4 mg, 41.3 μ mol) were placed in a 50 mL jacketed flask with 25.0 mL anhydrous CH_3CN . The flask was sealed, degassed with N_2 , and cooled to 5 $^\circ$ C with a circulating cooling bath. The reaction was photolyzed for 45 min with a 400 nm low-pass filter before the addition of $NaOH_{aq}$ (1 mol eq.). With formation of an insoluble red precipitate; the remaining solution was analyzed by ESI-MS. Analogous experiments were done with DDQ as described in text.

Small scale photochemical oxidations of **1** and **4**

These followed procedures described above. A stock solution of $[Ru(bpy)_2ttma][PF_6]$ was prepared from 17.0 mg (23.7 μ mol) in 5.0 mL anhydrous acetonitrile (4.75 mM); a sample of this solution (220 μ L, 0.924 μ mol) was mixed with 200 equivalents of MV^{2+} (4.76 mg, 0.185 mmol) in a purged quartz cell and irradiated for 15 min with a 400 nm low-pass filter. The reaction was then mixed with excess $NaOH$ (0.25 mL of 0.143 M) and examined by LCMS for characterization and quantification of products.

Conclusions

The dithiomaltol complexes **1** and **4** undergo photo-oxidation in the presence of electron acceptors, reactivity which stems from transitions localized on the ligand. These results suggest the use of dithiomaltol and hetero-substituted maltol derivatives for applications which require photo-induced electron transfers independent of redox-active metal ions.

Acknowledgements

This research was supported by the American Chemical Society (PJF PRF 51921-ND3) and NIH-NIGMS (MS 5SC1GM084776). MAO acknowledges support by the National Science Foundation (CHE-0911690; CMMI-0963509; CHE-0840518) and the Robert A. Welch Foundation (Grant B-1542). We thank Professors Jay Winkler and T. J. Meyer for helpful discussions.

References

- 1 N. Robertson, *Angew. Chem., Int. Ed.*, 2006, **45**, 2338–2345.
- 2 M. H. V. Huynh, D. M. Dattelbaum and T. J. Meyer, *Coord. Chem. Rev.*, 2005, **249**, 457–483.
- 3 B. Durham, S. R. Wilson, D. J. Hodgson and T. J. Meyer, *J. Am. Chem. Soc.*, 1980, **102**, 600–607.
- 4 J.-P. Collin, D. Jouvenot, M. Koizumi and J.-P. Sauvage, *Inorg. Chem.*, 2005, **44**, 4693–4698.
- 5 M. J. Bjerrum, D. R. Casimiro, I. J. Chang, A. J. Di Bilio, H. B. Gray, M. G. Hill, R. Langen, G. A. Mines, L. K. Skov and J. R. Winkler, *J. Bioenerg. Biomembr.*, 1995, **27**, 295–302.
- 6 J. K. Hurst, *Coord. Chem. Rev.*, 2005, **249**, 313–328.
- 7 P. K. Ghosh, B. S. Brunschwig, M. Chou, C. Creutz and N. Sutin, *J. Am. Chem. Soc.*, 1984, **106**, 4772–4783.
- 8 E. L. Lebeau, S. A. Adeyemi and T. J. Meyer, *Inorg. Chem.*, 1998, **37**, 6476–6484.
- 9 N. J. Cherepy, G. P. Smestad, M. Grätzel and J. Z. Zhang, *J. Phys. Chem. B*, 1997, **101**, 9342–9351.
- 10 W. Kandioller, A. Kurzwernhart, M. Hanif, S. M. Meier, H. Henke, B. K. Keppler and C. G. Hartinger, *J. Organomet. Chem.*, 2011, **696**, 999–1010.
- 11 M. Hanif, P. Schaaf, W. Kandioller, M. Hejl, M. A. Jakupec, A. Roller, B. K. Keppler and C. G. Hartinger, *Aust. J. Chem.*, 2010, **63**, 1521–1528.
- 12 É. A. Enyedy, O. Dömötör, E. Varga, T. Kiss, R. Trondl, C. G. Hartinger and B. K. Keppler, *J. Inorg. Biochem.*, 2012, **117**, 189–197.
- 13 S. Chaves, R. Jelic, C. Mendonça, M. Carrasco, Y. Yoshikawa, H. Sakurai and M. A. Santos, *Metallomics*, 2010, **2**, 220–227.
- 14 J. A. Lewis and S. M. Cohen, *Inorg. Chem.*, 2004, **43**, 6534–6536.
- 15 F. E. Jacobsen, J. A. Lewis and S. M. Cohen, *J. Am. Chem. Soc.*, 2006, **128**, 3156–3157.
- 16 K. Blazevic, K. Jakopcic and V. Hahn, *Bull. Sci., Sect. A*, 1969, **14**, 1.
- 17 J. A. Lewis, D. T. Puerta and S. M. Cohen, *Inorg. Chem.*, 2003, **42**, 7455–7459.
- 18 S. R. Schlesinger, B. Bruner, P. J. Farmer and S.-K. Kim, *J. Enzyme Inhib. Med. Chem.*, 2013, **28**, 137–142.
- 19 D. Brayton, F. E. Jacobsen, S. M. Cohen and P. J. Farmer, *Chem. Commun.*, 2006, 206.
- 20 M. Backlund, J. Ziller and P. J. Farmer, *Inorg. Chem.*, 2008, **47**, 2864–2870.
- 21 I. J. Chang, H. B. Gray and J. R. Winkler, *J. Am. Chem. Soc.*, 1991, **113**, 7056–7057.
- 22 M. M. Backlund Walker, *Unexpected reactivity of sulfur chelators*, Ph.D., University of California, Irvine, California, United States, 2009.
- 23 D. F. Brayton, *Targeting melanoma via metal based drugs: Dithiocarbamates, disulfiram copper specificity, and thiomaltol ligands*, Ph.D., University of California, Irvine, California, United States, 2006.
- 24 A. Petroni, L. D. Slep and R. Etchenique, *Inorg. Chem.*, 2008, **47**, 951–956.
- 25 H. Zhang, C. S. Rajesh and P. K. Dutta, *J. Phys. Chem. A*, 2008, **112**, 808–817.
- 26 (a) K. S. Alber, T. K. Hahn, M. L. Jones, K. R. Fountain and D. A. Van Galen, *J. Electroanal. Chem.*, 1995, **383**, 119–126;

- (b) D. M. Frank, P. K. Arora, J. L. Blumer and L. M. Sayre, *Biochem. Biophys. Res. Commun.*, 1987, **147**, 1095–1104;
- (c) N. Curtis, G. Lawrance and A. Sargeson, *Aust. J. Chem.*, 1983, **36**, 1327–1339; (d) S. Dileesh and K. R. Gopidas, *J. Photochem. Photobiol., A*, 2004, **162**, 115–120.
- 27 H. C. Smitherman and L. N. Ferguson, *Tetrahedron*, 1968, **24**, 923–932.
- 28 J. Jonas, W. Derbyshire and H. S. Gutowsky, *J. Phys. Chem.*, 1965, **69**, 1–5.
- 29 A. Saieswari, U. Deva Priyakumar and G. Narahari Sastry, *J. Mol. Struct. (THEOCHEM)*, 2003, **663**, 145–148.
- 30 M. DeRosa, *Coord. Chem. Rev.*, 2002, **233–234**, 351–371.
- 31 S. L. Murov and G. L. Carmichel, *Handbook of Photochemistry*, CRC Press, 1993.
- 32 A. Maciejewski, M. Szymanski and R. P. Steer, *Chem. Phys. Lett.*, 1988, **143**, 559–564.
- 33 M. Szymanski, R. P. Steer and A. Maciejewski, *Chem. Phys. Lett.*, 1987, **135**, 243–248.
- 34 S. Protti, A. Mezzetti, J.-P. Cornard, C. Lapouge and M. Fagnoni, *Chem. Phys. Lett.*, 2008, **467**, 88–93.
- 35 M. Borges, A. Romão, O. Matos, C. Marzano, S. Caffieri, R. S. Becker and A. L. Maçanita, *Photochem. Photobiol.*, 2002, **75**, 97–106.
- 36 W. Schlindwein, E. Waltham, J. Burgess, N. Binsted, A. Nunes, A. Leite and M. Rangel, *Dalton Trans.*, 2006, 1313–1321.
- 37 G. M. Sheldrick, *SHELXS97*, University of Gottingen, Germany, 1997.
- 38 G. M. Sheldrick, *SHELXL97*, University of Gottingen, Germany, 1997.
- 39 *SAINT-Plus*, Bruker AXS Inc., Madison, 2008.
- 40 G. M. Sheldrick, *SHELXTL*, Bruker AXS Inc., University of Gottingen, Germany, 2000.